

AFRL-SN-WP-TP-2002-108

**A STATIC TECHNIQUE FOR THE
ELECTRO-MECHANICAL
CHARACTERIZATION OF ORGANIC
MEMS DEVICES FOR RF AND
MICROWAVE APPLICATIONS**



Anupama B. Kaul, Tomasz Klosowiak, and Joshua Liu

MARCH 2002

Approved for public release; distribution is unlimited.

20020918 118

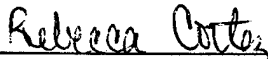
**SENSORS DIRECTORATE
AIR FORCE RESEARCH LABORATORY
AIR FORCE MATERIEL COMMAND
WRIGHT-PATTERSON AIR FORCE BASE, OH 45433-7318**

NOTICE

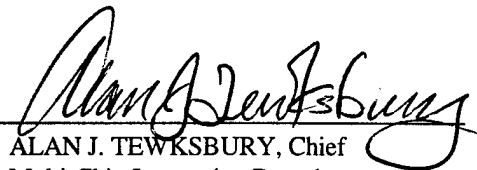
USING GOVERNMENT DRAWINGS, SPECIFICATIONS, OR OTHER DATA INCLUDED IN THIS DOCUMENT FOR ANY PURPOSE OTHER THAN GOVERNMENT PROCUREMENT DOES NOT IN ANY WAY OBLIGATE THE U.S. GOVERNMENT. THE FACT THAT THE GOVERNMENT FORMULATED OR SUPPLIED THE DRAWINGS, SPECIFICATIONS, OR OTHER DATA DOES NOT LICENSE THE HOLDER OR ANY OTHER PERSON OR CORPORATION; OR CONVEY AND RIGHTS OR PERMISSION TO MANUFACTURE, USE, OR SELL ANY PATENTED INVENTION THAT MAY RELATE TO THEM.

THIS REPORT HAS BEEN REVIEWED BY THE OFFICE OF PUBLIC AFFAIRS (ASC/PA) AND IS RELEASABLE TO THE NATIONAL TECHNICAL INFORMATION SERVICE (NTIS). AT NTIS, IT WILL BE AVAILABLE TO THE GENERAL PUBLIC, INCLUDING FOREIGN NATIONS.

THIS TECHNICAL REPORT HAS BEEN REVIEWED AND IS APPROVED FOR PUBLICATION.



REBECCA CORTEZ, Project Engineer
Multi-Chip Integration Branch
Aerospace Components & Subsystems Division



ALAN J. TEWKSBURY, Chief
Multi-Chip Integration Branch
Aerospace Components & Subsystems Division



ROBERT T. KEMERLEY, Chief
Aerospace Components & Subsystems Division
Sensors Directorate

IF YOUR ADDRESS HAS CHANGED, IF YOU WISH TO BE REMOVED FROM OUR MAILING LIST, OR IF THE ADDRESSEE IS NO LONGER EMPLOYED BY YOUR ORGANIZATION PLEASE NOTIFY AFRL/SNDL, WRIGHT-PATTERSON AFB, OH 45433-7322 TO HELP MAINTAIN A CURRENT MAILING LIST.

COPIES OF THIS REPORT SHOULD NOT BE RETURNED UNLESS RETURN IS REQUIRED BY SECURITY CONSIDERATIONS, CONTRACTUAL OBLIGATIONS, OR NOTICE ON A SPECIFIC DOCUMENT.

REPORT DOCUMENTATION PAGE				<i>Form Approved</i> OMB No. 0704-0188	
The public reporting burden for this collection of information is estimated to average 1 hour per response, including the time for reviewing instructions, searching existing data sources, gathering and maintaining the data needed, and completing and reviewing the collection of information. Send comments regarding this burden estimate or any other aspect of this collection of information, including suggestions for reducing this burden, to Department of Defense, Washington Headquarters Services, Directorate for Information Operations and Reports (0704-0188), 1215 Jefferson Davis Highway, Suite 1204, Arlington, VA 22202-4302. Respondents should be aware that notwithstanding any other provision of law, no person shall be subject to any penalty for failing to comply with a collection of information if it does not display a currently valid OMB control number. PLEASE DO NOT RETURN YOUR FORM TO THE ABOVE ADDRESS.					
1. REPORT DATE (DD-MM-YY) March 2002		2. REPORT TYPE Preprint		3. DATES COVERED (From - To)	
4. TITLE AND SUBTITLE A STATIC TECHNIQUE FOR THE ELECTRO-MECHANICAL CHARACTERIZATION OF ORGANIC MEMS DEVICES FOR RF AND MICROWAVE APPLICATIONS				5a. CONTRACT NUMBER F33615-00-2-1718	
				5b. GRANT NUMBER	
				5c. PROGRAM ELEMENT NUMBER 69199F	
6. AUTHOR(S) Anupama B. Kaul, Tomasz Klosowiak, and Joshua Liu				5d. PROJECT NUMBER ARPS	
				5e. TASK NUMBER ND	
				5f. WORK UNIT NUMBER OR	
7. PERFORMING ORGANIZATION NAME(S) AND ADDRESS(ES) Motorola Labs Advanced Technology Center Schaumburg, IL 60196				8. PERFORMING ORGANIZATION REPORT NUMBER AFRL-SN-WP-TP-2002-108	
9. SPONSORING/MONITORING AGENCY NAME(S) AND ADDRESS(ES) Sensors Directorate Air Force Research Laboratory Air Force Materiel Command Wright-Patterson Air Force Base, OH 45433-7318				10. SPONSORING/MONITORING AGENCY ACRONYM(S) AFRL/SNDI	
				11. SPONSORING/MONITORING AGENCY REPORT NUMBER(S) AFRL-SN-WP-TP-2002-108	
12. DISTRIBUTION/AVAILABILITY STATEMENT Approved for public release; distribution is unlimited.					
13. SUPPLEMENTARY NOTES Submitted for publication in the proceedings of the Spring 2002 Materials Research Society Meeting, held April 2002. This document was submitted to DTIC with color content. When the document was processed by DTIC, the color content was lost.					
14. ABSTRACT (Maximum 200 Words) An approach for measuring force-dependent properties of microscopic structures commonly found in MEMS has been developed. The system has the capability of measuring forces and deflections on the order of micro-newtons and micro-meters, respectively. By implementing a visual inspection system, force can be selectively applied to localized areas on a beam, and the resulting force-deflection characteristic obtained from which beam stiffness and effective elastic modulus can be calculated. These results were compared to simulation, which was performed using ANSYS FEM code. In addition, by applying a known mechanical force, direct correlation to voltage and thus electrostatic force can be obtained, which also elucidates the magnitude of the electrostatic feedback effect. Characterization of other force-dependent parameters such as contact resistance at DC, in addition to isolation/insertion loss at RF and microwave frequencies was obtained experimentally from which parameters such as lumped capacitance and inductance can be extracted.					
15. SUBJECT TERMS MEMS, RF, microwave, FEM modeling					
16. SECURITY CLASSIFICATION OF:			17. LIMITATION OF ABSTRACT: SAR	18. NUMBER OF PAGES 14	19a. NAME OF RESPONSIBLE PERSON (Monitor) Rebecca Cortez 19b. TELEPHONE NUMBER (Include Area Code) (937) 255-4557 x3449
a. REPORT Unclassified	b. ABSTRACT Unclassified	c. THIS PAGE Unclassified			

A static technique for the electro-mechanical characterization of organic MEMS devices for RF and microwave applications

Anupama B. Kaul, Tomasz Klosowiak, and Joshua Liu
Advance Technology Center, Motorola Labs,
Schaumburg, IL 60196, USA

ABSTRACT

An approach for measuring force-dependent properties of microscopic structures commonly found in MEMS has been developed. The system has the capability of measuring forces and deflections of the order of micro-newtons and micro-meters, respectively. By implementing a visual inspection system, force can be selectively applied to localized areas on a beam, and the resulting force-deflection characteristic obtained from which beam stiffness and effective elastic modulus can be calculated. These results were compared to simulation, which was performed using ANSYS FEM code. In addition, by applying a known mechanical force, direct correlation to voltage and thus electrostatic force can be obtained, which also elucidates the magnitude of the electrostatic feedback effect. Characterization of other force-dependent parameters such as contact resistance at DC, in addition to isolation/insertion loss at RF and microwave frequencies was obtained experimentally from which parameters such as lumped capacitance and inductance can be extracted.

INTRODUCTION

Microelectromechanical (MEMS) devices are revolutionizing every aspect of technology as we begin to realize the benefits of integrating micromechanical structures with electronics. A widely studied micromechanical structure is the cantilever beam, which was first demonstrated in 1979 to switch low-frequency electrical signals using electrostatic actuation [1]. The electrical performance of the cantilever beam switch is closely tied to the beam properties; for example actuation voltages or contact forces are directly dependent on beam stiffness and surface conditioning and the latter parameters can be easily influenced by processing. The MEMS designer would thus benefit from an empirical quantification of such properties in order to ensure device reliability and optimize performance. In addition to existing techniques for quantifying such properties of microscopic structures, for example nanoindenters [2] and AFMs, we describe an approach that accurately quantifies force-dependent electrical and mechanical properties of the cantilever beam switch, and could be used to analyze other MEMS structures. This paper describes the use of this system to quantify parameters such as beam stiffness and its comparison to mechanical simulation, effective elastic modulus, actuation forces, and contact forces at DC and frequencies up to 10 GHz. The extraction of lumped capacitances will also be discussed.

EXPERIMENTAL SET-UP

The schematic of the set-up which was developed to quantify micron-scale forces and deflections on localized areas of the MEMS cantilever beam is shown in Fig. 1a. A standard laboratory micro-balance registers the force with a resolution of 1 μN , and a precision dial-indicator mounted on a height gauge was used to monitor the deflection, which can be measured to a resolution of 0.6 μm . The force is delivered via a modified pogopin tip, which is on a fixture that is placed directly on the microbalance. By placing the height gauge on an x-y table, fine alignment of the force to a specific area on the beam can be performed. This alignment was enhanced by

magnifying the device features using a telescope, which is connected to a video imaging system and provides a view of the device in cross-section, while deformation takes place. After calibration, the height gauge is moved up, so that a deflection is registered on the dial-indicator; the corresponding force supplied to the beam as registered on the microbalance is then recorded. Electrical connections are made to the device using fine gauge wire such that contact resistance and actuation voltages can be measured simultaneously with the force and deflection data. Figure 1b is a typical image resulting from the optical/video system showing the force tip located directly above the end of the MEMS beam.

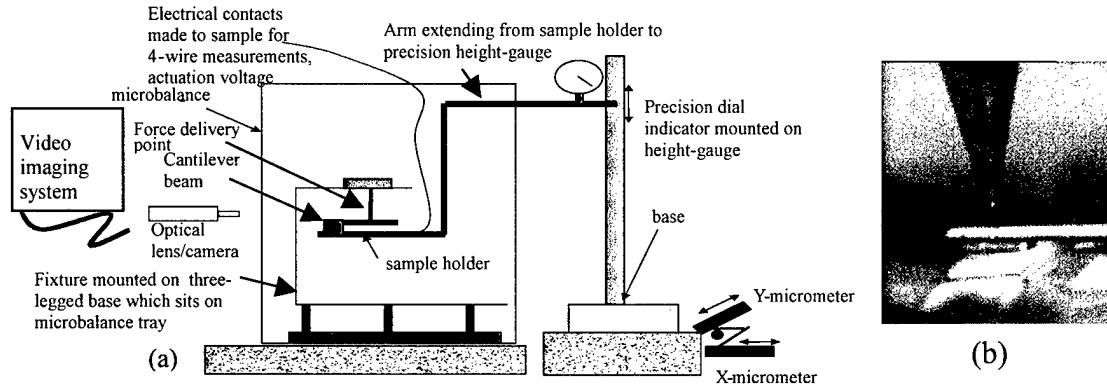


Figure 1. (a) Schematic of set-up for performing contact-force, contact-resistance measurements; (b) the tip of the force delivery point shown located above the end of the MEMS beam.

RESULTS AND DISCUSSION

Stiffness determination

The repeatability error associated with the measurement system was determined to be 2%. Figure 2a depicts the force-deflection characteristic of a cantilever beam over 6 loadings. With the force applied at the end of the beam as shown in Fig. 1b, the stiffness k of the beam was obtained from the slope of this graph, and an average k of $1.56 \text{ N/m} \pm 0.03 \text{ N/m}$ ($1-\sigma$) was determined. This system was then used to characterize the k of several beam geometries. For example, the k of two structures can be calculated from Fig. 2b. The force was applied at the center of the capacitor electrode, which is some distance between the anchor and the free-end of the beam. A k value of 6.5 N/m and 2.5 N/m was calculated for structure 1 and structure 2, respectively, which confirms the notion that structure 1 is stiffer and would thus have a higher actuation voltage; this is consistent with the findings in [3]. Simulation results will be presented shortly.

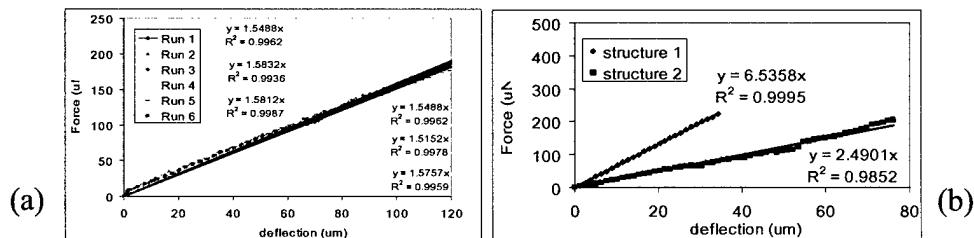


Figure 2. (a) Determination of beam stiffness and repeatability; (b) spring constant of two structures.

If the force-deflection characteristic is extended to higher deflections, 3 distinct regimes emerge as indicated in Fig. 3a. The slope of the first region depicts the stiffness of the beam alone, similar to Fig. 2b. The second steeper region is believed to arise from the contact pad engaging the

signal traces. The third, highest slope region is where the top capacitor electrode has touched the substrate and is reflective of the stiffness of the measurement assembly, which was determined to be 12.7 kN/m from a calibration run; this is several orders of magnitude larger than the stiffness of the device. To the MEMS designer, the second region would be of significant interest since it provides a way to quantify the system stiffness when the contact pad has engaged the signal trace. This can be especially beneficial when two devices that have different contact pad materials are characterized as shown in Fig. 3a. With material A comprising the contact pad, the system stiffness when this contact pad touches the signal trace is determined to be 108 N/m. This is to be compared with the second device that has a contact pad made of material B, which results in a stiffness of 196 N/m. This appears to be consistent with the fact that the elastic modulus of material B is double when compared to that of material A, and so the latter case would result in a lower stiffness as is observed. Therefore, the set-up can be used to quantify system stiffness of varying materials that are located at different points on the beam.

It should be pointed out that the stiffness of the first region in Fig. 3a, which refers to the beam alone, is the same in both cases ~ 6.5 N/m. From a knowledge of k , the effective elastic modulus E of the beam can be derived and is given in Eqn. 1:

$$E = \frac{12kl \left(\frac{l^2}{3} + la + a^2 \right)}{wh^3} \quad (1)$$

where l , w , h , $2a$ are the beam length, width, thickness and length of the capacitor electrode, respectively. Note that this equation reduces to the straight cantilever beam fixed at one end case if $a = 0$. Given typical parameters of the beam, the effective elastic modulus E was calculated to be ~ 101 GPa from a measured k of 6.5 N/m.

This set-up can also be used to characterize the thermal response of MEMS devices. When currents of the order of hundreds of mA at power levels of ~ 1 W are applied for some duration through the signal pads with a known mechanical force at the contact pad, the pad area is seen to geometrically distort. The force-deflection characteristic, shown in Fig. 3b, reveals this distortion since the contact pad appears to touch the signal trace at a smaller deflection. The slope of the second region, attributed to the contact pad, results in a stiffness change of less than 11 %, from 108 N/m before to 121 N/m after current application. This slight increase could be due to initial signs of aging, resulting from material hardening due to Joule heating. Such a system can thus be used to characterize the thermal response of MEMS devices under controlled conditions.

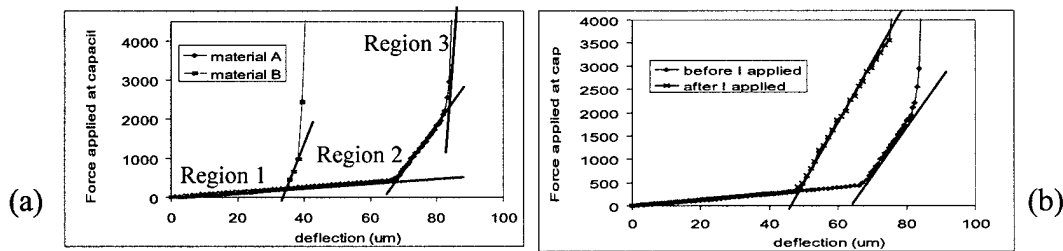


Figure 3. (a) Comparison of stiffness of two contact pad materials; (b) change in stiffness observed after joule heating.

ANSYS simulation

Given the geometrical parameters of the straight beam device for which the measured data is shown in Fig. 2, an ANSYS model was constructed and the stiffness of various regions was determined from simulation and compared to the experimentally obtained values. The shell model and FEM analysis was used, and electrostatic force f_e was calculated using the equation for the

capacitor with two infinite parallel metal plates. The stiffness results are summarized in Table 1, which indicates the boundary conditions (BC) and load configurations. In case (iii), the force was applied at the capacitor electrode.

Table 1. Comparison of stiffness values between simulation and measurement

BC and load configuration	k (N/m)-simulated	k (N/m)-measured	% difference
(i) k_{beam} - force applied at capacitor	1.6	1.5	6
(ii) k_{beam} - force applied at contact pad	6.4	6.5	1.5
(iii) k_{system} (with contact pad engaged)	51	108	52

In general, the simulation value for the stiffness appears to be in close agreement to the measured values as shown in the last column of Table 1. The largest difference is in the stiffness of the system with contact pad engaged (iii). This may be because several assumptions were made, such as the true contact area being exactly equal to the overlap area at the signal traces. More work is necessary to isolate the reason for this difference.

ANSYS/Multiphysics was also used to model two types of devices that have geometries similar to structure 1 and structure 2 of Fig. 2b. The ratio of f_e to δ_c , where δ_c is the displacement at the capacitor center after a force f_e is applied there, was calculated as the overall k. In this case, $k_{\text{structure-1}}$ is determined to be 2.51 N/m and $k_{\text{structure-2}}$ is 1.61 N/m. These simulation results agree qualitatively with the trend observed experimentally that structure 1 is less stiff compared to structure 2, as determined from Fig. 2b.

Actuation voltage and the electrostatic feedback effect

This set-up was also used to perform unique experiments to determine the direct equivalence of voltage to absolute electrostatic force. In this particular case, the device was pre-deflected at the capacitor electrode to a known value and the corresponding force applied to the device was recorded from the balance. A voltage was then applied between the capacitor electrodes to initiate electrostatic actuation. The mechanical force on the balance was seen to decrease as the voltage increased. A family of curves results, shown in Fig. 4a, which shows the exact correspondence of mechanical force to voltage and hence electrostatic force for various levels of increasing initial loads.

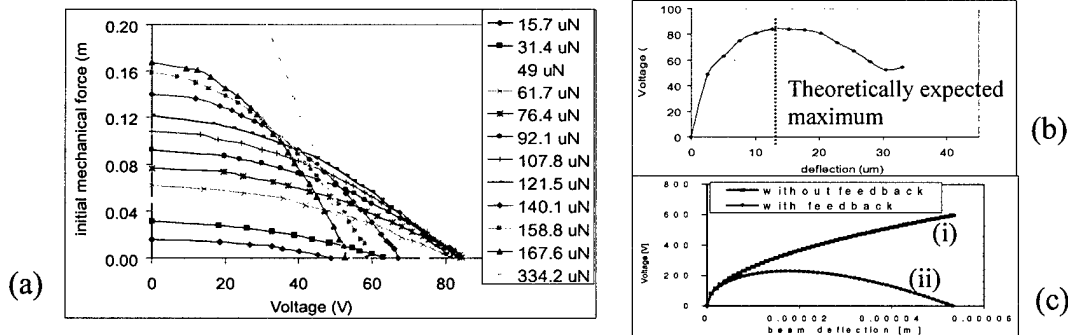


Figure 4. (a) Correlation between force and voltage; (b) voltage as a function of gap for measured device; (c) simulation results depicting the effect of the electrostatic feedback effect.

It should be apparent that the maximum voltage observed is about 82 V, which is the actuation voltage of this device; when the device is artificially deflected to distances beyond $d/3$, where d is the deflection of the beam, the system responds by self-actuating at voltages less than 82 V. During dynamic operation, the 82 V would be referred to as the pull-in voltage. From Fig. 4b,

which shows the voltage as a function of deflection at the capacitor electrode, it can be verified that the electrostatic feedback effect is indeed operative. Fig. 4c shows simulation results that compares the 2 cases: (i) electrical force not dependent on gap but on V only, and (ii) electrical force dependent on voltage and gap which can be referred to as the electrostatic feedback effect. The force increase leads to a gap decrease and the gap decrease causes the force to increase. The curve in (ii) reflects physical reality and this agrees with experimental observations, as shown in Fig. 4b. Moreover, the maximum voltage in Fig. 4b occurs at approximately $d/3$, which is consistent with the theoretical predictions of Fig. 4c. In addition, an actuation voltage of 82 V corresponds to a force of 92 μN , which appears in agreement, to first order, with simulation.

Contact resistance – contact force measurement

This set-up was also used to measure contact forces necessary for electrical closure to occur at the contact pad. Figure 5 shows the force-deflection-resistance characteristic for a beam with the force applied at the end of the beam or contact pad. From this it can be deciphered that electrical contact is achieved in the steeper portion of the curve shown in (i), at some point after the contact pad has first touched the signal traces. The extra force beyond initial contact or the net contact force is indicated as ΔF when initial conductivity, shown by curve (ii), is first observed. With an increase in ΔF beyond 200 μN , the resistance is seen to sharply decrease with force, until an equilibrium value is reached which results in a contact resistance of less than 60 $\text{m}\Omega$. This decrease in resistance with force has been observed in the past [4, 5] and is attributed to an increase in the contact area of surface asperities, which plastically deform until the constriction resistance is finally attained [6]. Using this set-up the MEMS designer can thus benefit from a knowledge of the actual contact forces necessary, which is a unique function of geometry and surface conditioning, to ensure DC conductivity.

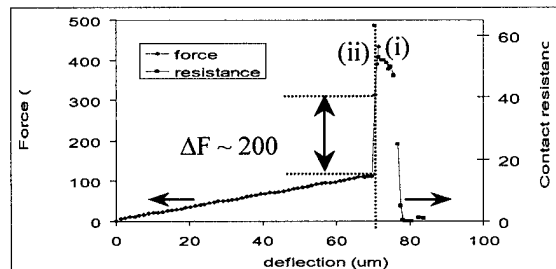


Figure 5. Force-deflection-resistance characteristic for a device indicating extra force beyond initial contact is required for DC conductivity.

Contact force measurements for RF

Besides DC measurements, the set-up was adapted such that electrical measurements could also be performed at high frequency. A network analyzer was used with a high-frequency test fixture which consisted of microstrip edge terminations that were spring loaded and could be connected to the transmission lines on the substrate; these lines were designed to have an impedance of 50 Ω on the particular substrate on which the MEMS device was fabricated. This test fixture was mounted on the force-deflection system using a specially designed holder, in much the same way as shown in Fig 1a. Ports 1 and 2 of the Network Analyzer were connected to the input and output RF lines of the MEMS device.

S-parameter data was gathered as a function of deflection and force applied at the contact pad. Fig. 6a shows the isolation and insertion loss as a function of frequency up to 10 GHz for 3 force levels. As force is applied to the free end of the beam, the gap decreases which decreases the

isolation. In this case, a particularly large force is required to bring the switch to the insertion loss state and may have to do with the surface characteristics of this particular device. Figure 6b shows the isolation/insertion loss as a function of gap for 3 frequencies which suggests that the isolation becomes worse at higher frequencies. This data also indicates that the gap appears to have little influence on isolation for gaps beyond about 50 μm at these frequencies; below 50 μm the isolation decreases rapidly with gap. By modeling S-parameter data according to Eqn. 2 obtained from [7],

$$|S_{21}|^2 = 4\omega^2 C_u^2 Z_0^2 \quad (2)$$

where ω , C_u , and Z_0 are the frequency, capacitance and characteristic impedance, respectively, the

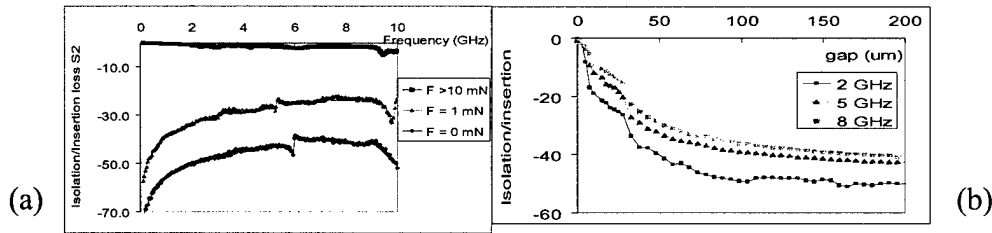


Figure 6. (a) Isolation/insertion loss as a function of (a) frequency for 3 forces, resonances are also observed; (b) gap for 3 frequencies.

capacitance C_u can be extracted as a function of gap; for example, in the off-state a net capacitance of 10 fF was calculated. Also shown in Fig. 6a are resonances which occur between 4 – 6 GHz and above 9 GHz. The resonances in either band tend to shift to a lower frequency when higher force is applied, which would decrease the gap. This seems consistent with what is expected, as a reduced gap leads to an increased capacitance, which would decrease f_R according to Eqn. 3,

$$f_R = \frac{1}{2\pi\sqrt{LC}} \quad (3)$$

Given the location of f_R the inductance can be calculated by which was determined to be ~ 70 nH in the open state. Therefore, such a system allows parameters such as lumped capacitances and inductances to be determined as a function of gap and force, which can be of extreme benefit to the MEMS designer.

SUMMARY AND CONCLUSIONS

A simple, flexible and accurate technique was developed and described that allows the measurement of micro-newton forces and deflections of MEMS structures. Several examples were highlighted where force-dependent mechanical and electrical parameters were obtained using this set-up. The empirical knowledge of these parameters is of extreme benefit to the MEMS designer in order to design devices that operate reliably. Such information can ultimately be used to optimize device performance.

ACKNOWLEDGEMENTS

We would like to thank Manes Eliacin and Rajnikant Desai for fabricating the organic MEMS devices and Dr. Keryn Lian, Robert Lemkowski and Marc Chason for their support and useful discussions. We also acknowledge the support of DARPA grant # F33615-00-2-1718.

REFERENCES

- [1] K. Petersen, "Micromechanical membrane switches on silicon," *IBM J. Res. Develop.*, vol. 23, pp. 376-385, 1979.
- [2] J. L. Hay and G. M. Pharr "Instrumented indentation testing," pp. 232-243.
- [3] S. P. Pacheco, L. P. B. Katehi, and C. T.-C. Nguyen, "Design of low actuation voltage RF MEMS switch," *IEEE MTT-S Digest*, pp. 165-168, 2000.
- [4] S. Majumder, N. E. McGruer, P. M. Zavracky, G. G. Adams, R. H. Morrison, J. Krim, "Measurement and modeling of surface micromachined, electrostatically actuated microswitches," *Transducers '97*, pp. 1145-1148, June 1997.
- [5] D. Hyman and M. Mehregany, "Contact physics of gold microcontacts for MEMS switches," *IEEE Trans. on Comp. and Pack. Tech.*, vol. 22, no. 3, pp. 357-364, September 1999.
- [6] R. Holm, *Electric Contacts Handbook*, 4th Ed. Berlin, Germany: Springer-Verlag, 1967.
- [7] G. M. Rebeiz and J. B. Muldavin, "RF MEMS switches and switch circuits," *IEEE Microwave Mag.*, pp. 59-71, December 2001.